Acta Ophthalmologica

Assessing bulk emulsification at the silicone oil – saline solution interface in a 3D model of the eye

Ru Wang,[1] Martin Snead,[2] Philip Alexander[2] and D. Ian Wilson[1]

[1]Department of Chemical Engineering and Biotechnology, University of Cambridge, Cambridge, UK
[2]Addenbrooke's Hospital, Cambridge University Hospitals NHS Foundation Trust, Cambridge, UK

ABSTRACT.

Purpose: **Emulsification of silicone oil (SiOil) in a vitrectomized eye was investigated using a 3D model of the vitreous cavity to test the hypothesis that oil droplet formation arises from the breakdown of the bulk SiOil-aqueous interface during eye saccadic movement.**

Methods: **Round bottom flasks filled with SiOil and a saline phase modelled the vitrectomized SiOil-filled eye. A stepper motor imposed saccadic movements and the oil/aqueous interface was monitored with digital cameras. A range of SiOil viscosities, flask diameters, motion scenarios and levels of fill were studied. Estimates of velocity profiles in the fluid on the equatorial plane of a sphere subject to saccadic motion were obtained from an analytical solution to the Navier-Stokes equations.**

Results: **Interfacial waves were observed at saccadic motions with higher acceleration, amplitude and frequency. Low interfacial tension between the two fluids, lower oil viscosity and smaller level of SiOil fill all promoted large deformations of the interface. No droplets were formed at the bulk SiOil-aqueous interface. However, formation and detachment of oil droplets were observed at the three-phase contact line under certain conditions.**

Conclusions: **The stresses generated at the liquid-liquid interface are not large enough to form droplets in the bulk region for conditions representative of these in the eye. Bulk emulsification of the SiOil, reported as the main formation mechanism by some workers, is not responsible for droplet formation in a vitrectomized SiOil-filled eye set-up. This result confirms recent finding on droplet formation driven by a surface emulsification mechanism.**

Key words: emulsification – eye – fluid dynamics – interface stability – retinal detachment – silicone oil

Acta Ophthalmol. 2021: 99: e209–e214

doi: 10.1111/aos.14539

Introduction

Silicone oil (SiOil) is often used as a retinal tamponade in vitrectomized eyes to repair retinal detachment (Cibis et al. 1962; Kanski & Daniel. 1973). However, SiOil is prone to emulsification under the saccadic motion of the eye, resulting in impairment or loss of vision (Federman & Schubert 1988; Miller, Papakostas & Vavvas 2014). Oil emulsification has been attributed to the stresses generated at the interface between the oil and intraocular aqueous phases by such motion being large enough to disrupt the interface, overcoming the surface tension which tends to minimize the interfacial area (De Silva, Lim & Schulenburg 2005; Caramoy et al. 2015). If this bulk emulsification mechanism is correct, the properties of the SiOil, specifically the kinematic viscosity and interfacial tension, can be used to determine the likelihood of emulsification.

Previous studies have investigated the emulsification of SiOil in aqueous solution using cylindrical vials or glass cuvettes, and using various methods to mix the two phases (e.g. vortex, orifice homogenizers and sonication) (Nakamura, Refojo & Crabtree 1990; Caramoy et al. 2010). The results showed the effect of chemical composition, viscosity and other properties of the oil on the stability of the interface, but the geometries used were not representative of the eye shape and motion. In other studies, the eye chamber was modelled as a spherical cavity in a Perspex™ block (Bonfiglio et al. 2015), or as a cylindrical chamber made of acrylic glass coated with albumin proteins to simulate the hydrophilic retinal surface (Wetterqvist et al. 2004; Chan et al. 2011). The authors investigated the movement of a single fluid phase within this chamber and the movement of the oil relative to the aqueous and to the chamber wall, respectively. These studies provided insights into the motion at the wall and between the two fluids. Chan et al. used a 2D cylindrical model of the eye cross-section filled with oil and subject to a saccadic motion (10° amplitude, 390°/s

angular velocity, 950 ms latency time) and observed droplet formation for oils with different viscosity (from 5 to 5000 cSt) after running the test continuously for one to four days (Chan et al. 2015).

However, the difference in flow patterns in oscillating cylinders and spheres means that the results do not compare exactly and require verification. While numerical simulations of transient flow patterns in the eye exist (Abouali et al. 2012), these have not to date considered the presence of a liquid-liquid interface, partly due to the computational effort involved and the challenge of modelling a moving contact line. An experimental approach has therefore been employed here, supported by insights from earlier fluid mechanical analyses. The stability of the interface between the two phases in a 3D model of the eye chamber is investigated for liquid properties and motions representative of those arising in practice.

Materials

Oil and aqueous

Three chemical grades of silicone oil, labelled A500 (Sigma Aldrich), B1000 and B5000 (both Fischer Scientific) were studied. Saline solutions were prepared using de-ionized water and laboratory analytical grade salts: calcium chloride (3 mM, Fisher Scientific), magnesium chloride (1 mM, Fisher Scientific), sodium acetate trihydrate (30 mM, Alfa Aesar), sodium citrate tribasic dihydrate (15 mM, Sigma Aldrich), sodium chloride (111 mM, Fisher Scientific) and potassium chloride (10 mM, Sigma Aldrich). The pH of each batch of saline solution was adjusted to 7.4 using analytical grade hydrochloric acid (Fisher Scientific). Albumin protein from egg white (Sigma) and TX-100 surfactant solutions (Fluka) were prepared in saline at 1 wt. % concentration, which is above the critical micelle concentration for both solutions. Table 1 summarizes the physico-chemical properties of these working fluids. Liquid densities and surface tensions were measured using a pycnometer and a goniometer, respectively. A controlled stress rheometer confirmed that all liquids were Newtonian with constant viscosity. In certain cases, the working fluids were dyed to enhance visibility of the interface; oils were dyed with Oil Red O (Sigma Aldrich) and aqueous solutions with fluorescein sodium salt (Sigma Aldrich).

Table 1. Measured and calculated properties of working fluids at room temperature (20°)

				Silicone oils		
	Saline	1% Albumin	1% TX-100	A500	B1000	B5000
Density (± 1 kg/m^3)	1008	1010	1007	974	973	976
Surface tension, liquid-air (± 2 mN/m)	73	37	31	18	19	19
Viscosity (Pa s)	0.0017	0.0018	0.0022	0.51	0.92	4.66
	± 0.2 mPa s			$\pm$ 0.02 Pa s		
Kinematic viscosity (mm^2/s)	1.7	1.8	2.2	520	950	4770

The interfacial tension (IFT) between the saline solution and the silicon oils was around 28 mN/m and was reduced by the addition of surfactant. The IFT for aqueous solutions and oil B1000 was determined as 2.5 mN/m and 4.4 mN/m ($\pm$ 0.5 mN/m) for 1% albumin and 1% TX-100, respectively. The contact angle at the three-phase oil-aqueous-glass substrate interface without surfactant was 132° and increased to 164° and 163° (± 2°) for 1% albumin and 1% TX-100, respectively. These angle values are close to the value (162°) reported for silicone oil against the eye's retina in protein solutions (Fawcett, Williams & Wong, 1994). Experiments were performed with surfactant-free and surfactant-loaded solutions to cover the range of IFTs expected to arise in practice.

Eye chamber model and sample preparation

The eye chamber model utilized laboratory grade round bottom flasks (RBFs) of volume 5, 10 & 25 ml, with average radius equal to 12.5, 15 and 20 mM, thereby spanning the range of adult human eyes. The surgical procedure of replacing vitreous humour aims to fill the eye with SiOil completely so high levels of fill (>90 vol%) were investigated. Oils with density less than water were studied, allowing the system to be set in motion from above and cameras to focus on the base of the flask.

The internal glass surface was coated with albumin by filling the flask with 1% albumin solution for an hour or more. The albumin solution was then discarded, and the desired volume of aqueous (saline or 1% TX-100) introduced carefully to the base and washed across the surface, to wet it. SiOil was then introduced using a needle located at the centre of the flask above the aqueous layer. Care was taken to avoid air bubbles in either phase or unwanted mixing. Figure 1a shows a photograph of a sample with 96 vol% SiOil fill level.

Interfacial stability under saccadic motion

The filled RBF was attached to a stepper motor, as shown in Fig. 1b & c. The motor was connected to a microcontroller, which drove a simulated eye saccadic motion. Eye saccades are rapid movements of the eye that change the point of fixation followed by a rest time (Bahill, Clark & Stark, 1975). Saccades were represented here with alternate rectangular pulses of duration D and latency time L between each pulse (Fig. 2a). The amplitude of the saccade, A, was varied from 5.4° to 54° which covers the main range of human saccadic eye movements (Bahill, Clark & Stark, 1975). The maximum angular velocity, ω_{max}, was set at 200, 400, 600 or 800°/s. D was set by $\frac{A}{\omega_{max}}$, both being defined previously, and the influence of latency time was investigated with L values of 200 ms (average for an adult), 0.5D, D or 3D. We define a full saccade as the two alternate consecutive pulses, and the motion is periodic with a period T, with $T = 2(L + D)$.

The RBF was immersed in a mineral oil bath to reduce refraction effects, and the oil-aqueous interface was recorded for 3 min using a video camera with a long focal length lens. ImageJ (NIH, Bethesda, Maryland) was used to measure the interface length at rest, l_0 (Fig. 1d) and during motion, l_m, (Fig. 1e). The maximum

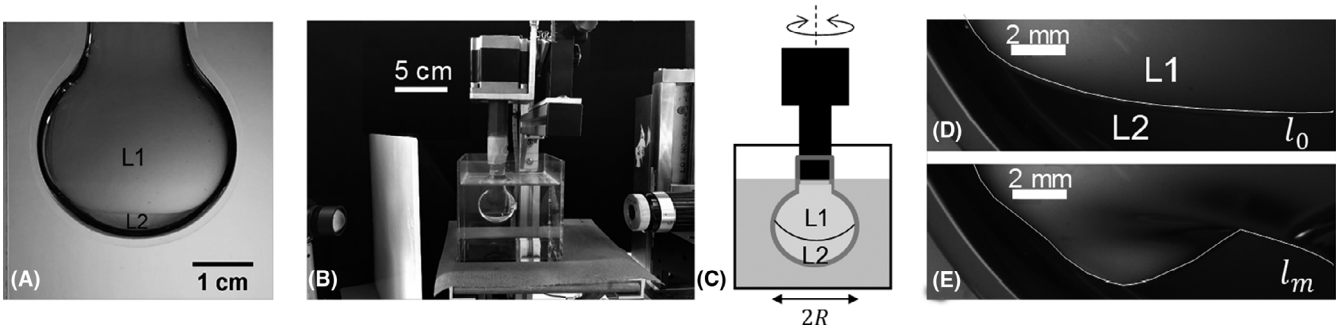

Fig. 1. (A) Photograph of a 10-ml RBF filled with silicone oil (L1) and saline (L2). (B) Photograph of the RBF attached to the stepper motor and immersed in a mineral oil bath, with the illuminating light on the left and camera lens on the right. (C) Schematic representation of the RBF sample attached to the motor. (D) Zoomed view of the oil-aqueous interface highlighted with a white line at rest, and (E) during saccadic motion with A = 36°,ω_{max} = 600°/s and L = 0.5D.

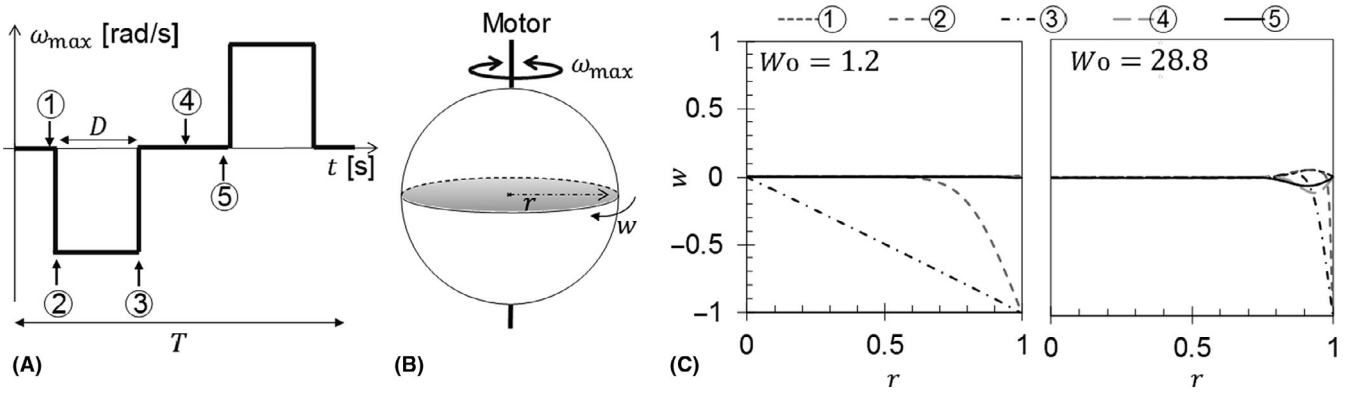

Fig. 2. (A) Saccade motion represented as alternate rectangular pulses of duration D, maximum angular velocity, ω_{max}, latency time, L, and period, T. (B) Sketch of the geometry involved and the equatorial plane highlighted in grey. (C) Calculated azimuthal velocity on the equatorial plane along the radius (centre of sphere $r = 0$, wall $r = 1$) at the five times marked on (A) for a single-phase B1000 oil ($Wo = 1.2$) and saline ($Wo = 28.8$) when A = 5.4°, ω_{max} = 200°/s, L = 0.2s.

length ratio, Δl^*, was calculated from

$$\Delta l^* = \frac{|l_m - l_0|}{l_0} \qquad (1)$$

Longer tests were run, for up to 3 days, for selected cases where Δl^* was large. These extended tests did not change Δl^* significantly nor result in bulk droplet formation.

Estimation of fluid velocity

Repetto, Siggers & Stocchino (2008) reported an analytical approach to calculate the motion of a viscous liquid within a spherical container subject to a sinusoidal planetary rotation with no slip at the wall. We adapted this approach to calculate the velocity profile on the equatorial plane when the driving motion took the form of a square wave, Fig. 2a, for a sphere filled with SiOil or with aqueous phase, to compare the resultant flow patterns. The square wave was expressed as a Fourier series, and the solution to the governing equations was obtained by combining the response to each component of the Fourier series. A more detailed description is given in the Supplementary Information.

Results

The motion induced by the glass wall depends on the Womersley number, Wo, which relates the magnitude of fluid inertia to the viscous forces in the flow:

$$Wo = \sqrt{\frac{R^2 \omega_{max}}{\nu}} \qquad (2)$$

Here, R is the flask radius and ν is the kinematic viscosity of the liquid. Figure 2c shows the simulated velocity profiles for a single-phase fluid in a spherical chamber at five sample times. For the case of saline (low ν, high Wo), there is little movement except near the wall throughout the cycle, whereas for the SiOil (high ν, low Wo), the wall motion penetrates the fluid interior because of viscous drag. When the chamber contains the two liquid phases, we can infer that distant from the interface and the wall the aqueous layer is almost static, whereas the oil moves from the wall towards the centre, generating a circulating pattern in the vertical plane. Figure 1e shows the formation of a buckled interface at the oil-aqueous interface under a saccade motion. The oil phase is shearing the quasi-stationary aqueous phase, and the difference in velocity is significant enough to generate the condition for the oscillatory Kelvin-Helmholtz instability (Yoshikawa et al. 2011). It is not, however, sufficiently large to disrupt the interface in this case.

When the RBF is oscillated above a certain threshold, the oil-aqueous

interface deforms and generates interfacial waves. The maximum length ratio, Δl^*, describes the extent of the deformation. Figure 3 shows the effect of different saccade conditions on Δl^* for the B5000 SiOil and saline in the absence and presence of surfactant. The oil B5000 – aqueous interface deforms noticeably ($\Delta l^* > 10$) when T is small. This is the case when (i) ω_{max} is high, corresponding to greater wall-driven inertia (and difference in velocities in the two phases), and (ii) low latency: the flow pattern in the fluid has not completely dissipated before the next pulse starts. The latter aspect is illustrated in Fig. 4a, which shows the effect of latency time on the velocity profile in the single-phase case. When T is large, there is insufficient time to dissipate inertia and for the fluid to come to rest before the next pulse begins, generating motion in the opposite direction and promoting interface instability. Data points with similar T give noticeably different Δl^*, which is due to the difference in saccade amplitude: at higher A, a greater proportion of the fluid layer was set in motion, resulting in higher Δl^* (Fig. 4b). Comparing the plots in Fig. 3, it can be seen that adding surfactant to the aqueous phase increased Δl^*, associated with reducing the IFT and making the interface more deformable and potentially unstable.

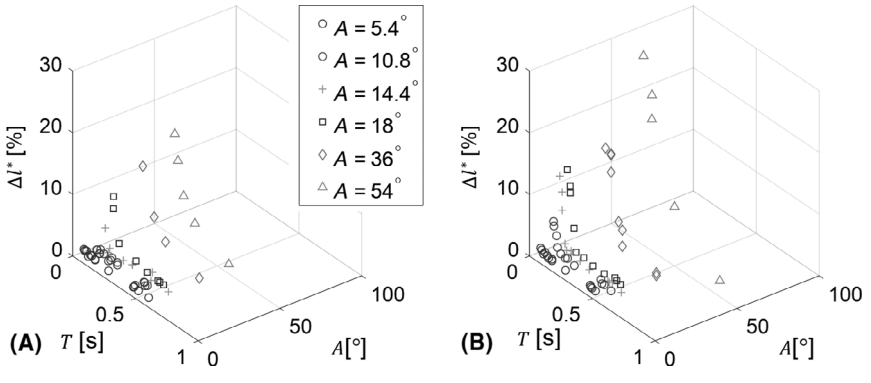

Fig. 3. Effect of saccade period and saccade amplitude on the maximum length ratio for a coated 25-ml RBF filled with 91 vol% B5000 SiOil and 9 vol% (A) pure saline; (B) 1 wt. % TX-100 in saline.

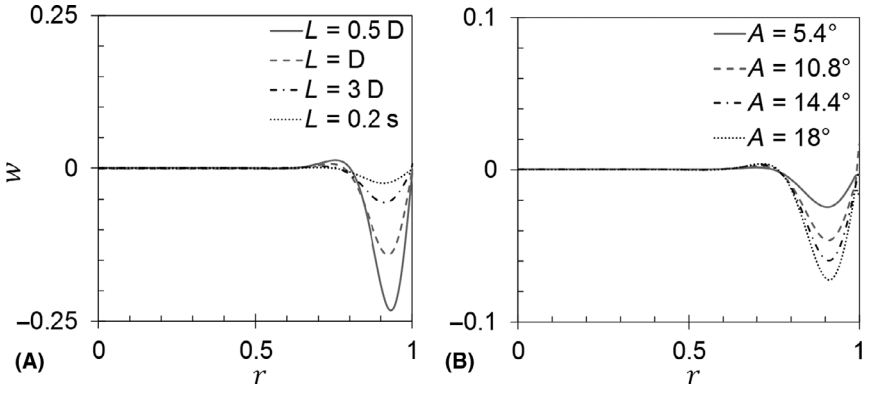

Fig. 4. Azimuthal velocity profiles on the equatorial plane along the radius of a single saline phase ($Wo = 28.8$) in a sphere, calculated at the 5th sample time defined in a. Saccade parameters were as follows: (A) A = 5.4°, ω_{max} = 200°/s, variable L. (B) ω_{max} = 200°/s, L = 0.2s, variable A.

The same trends were observed for all the combinations of SiOil and aqueous phase tested. Figure 5 shows the effect of oil viscosity, RBF volume and oil level of fill on the interface extension for surfactant-laden saline: pure saline gave smaller Δl^* values. For a given saccadic motion, Fig. 5a shows that a more viscous SiOil gave a less stable interface. This is the result of the interfacial tensions being similar (see Table 1) but the more viscous SiOil transfers the wall motion further into the chamber. Tests with different flask volumes did not show a significant difference (Fig. 5b), while increasing

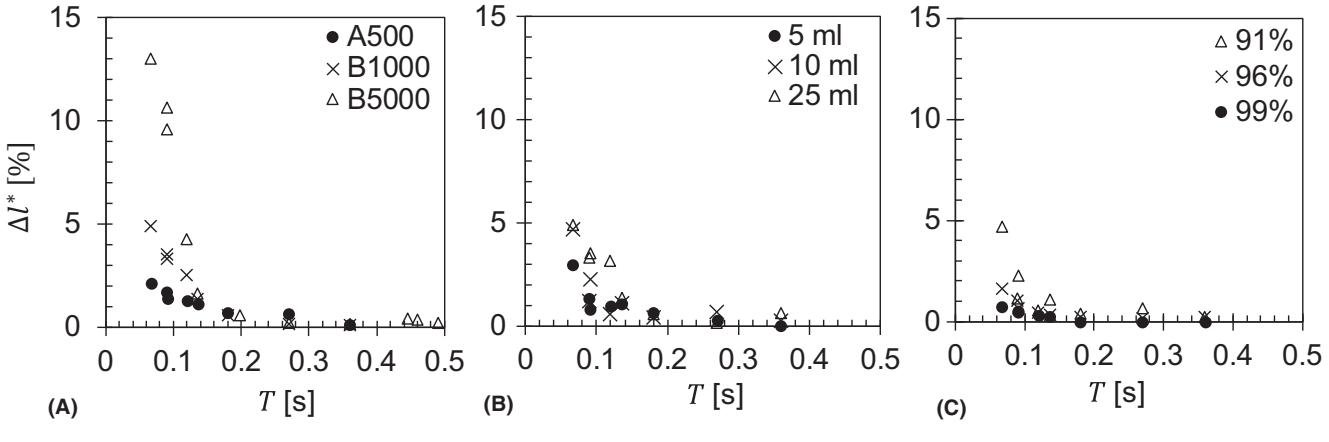

Fig. 5. Effect of oil viscosity, flask size and SiOil fill on the stability of the SiOil-aqueous (1% TX-100) interface. The amplitude of saccades was fixed to 18° for all experiments. (A) 25-ml RBF filled with 91 vol. % SiOil; (B) Different RBFs with 91 vol% B1000; (C) 10-ml RBF, different fill levels of B1000.

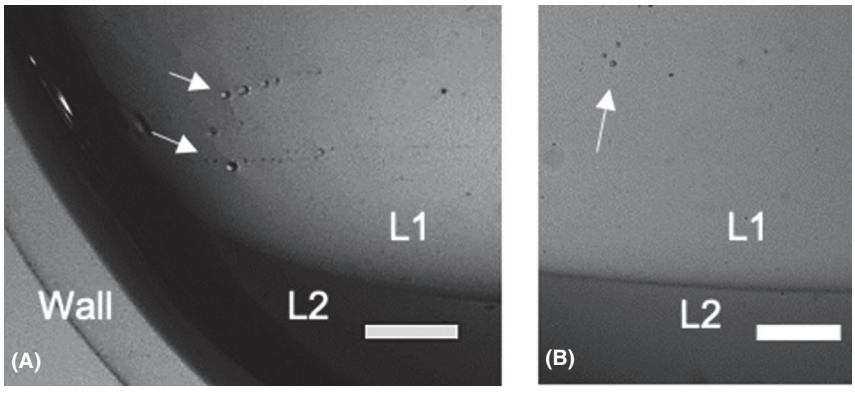

Fig. 6. Photographs of oil droplets (indicated by arrows) formed near the moving contact line: (A) 25 ml RBF with 91 vol% B5000 oil/1 wt% TX-100, saccade parameters (A = 54°, ω_{max} = 800°/s and $L = 0.5D$). (B) 25 ml RBF with 91 vol% B1000 oil/ 1 wt% TX-100, saccade parameters (A = 5.4°, ω_{max} = 400°/s and $L = 0.5D$). Scale bar = 2 mm. L1 = oil phase. L2 = aqueous phase.

the volume of SiOil improved the stability of the interface (Fig. 5c).

Droplet formation at the bulk SiOil-aqueous interface was not observed under any of the conditions tested in this work.

For certain combinations of saccadic motion parameters, SiOil type and fill, the formation of oil droplets was observed within the aqueous phase at the moving oil/aqueous/glass contact line (see Fig. 6). Near the glass wall, a thin layer of aqueous fluid is dragged back and forth, causing the contact line to move. Deformation of the contact line over the course of the saccade resulted in detachment of oil droplets after which subsequently moved into the aqueous phase where they remained.

Discussion

Emulsification of silicone oil is a common post-surgical complication with low viscosity oils (Federman & Schubert, 1988) and previous studies have suggested that droplet formation results from the shearing motion at the oil/aqueous interface and the break-up of the bulk oil phase. Chan et al. studied the effect of the eye motion on the interfacial shear stress in a 3D eye model (Chan et al. 2011). They studied two sets of saccadic motion (A = 9°, ω = 390°/s, D = 50 ms and A = 90°, ω = 360°/s, D = 300 ms) and did not report droplet formation in either case. This study has investigated a wider range of saccadic motions, chamber sizes and SiOils, covering the cases likely to arise in the eye (and extreme cases). There was no significant influence of chamber size on the stability of the interface. In all cases, bulk emulsification was not observed. The absence of droplet formation is consistent with the literature on viscous fingering, in which the flow of a less viscous liquid into a more viscous one (driven by an upstream pressure) promotes penetration of the more viscous liquid by the less viscous one via the Saffman-Taylor instability and can result in droplet formation (Saffman & Taylor 1958). When a more viscous liquid moves into a less viscous one, as occurs here, fingering does not occur.

It has been shown here that the transients induced by the saccadic motion do not generate enough inertia to overcome the interfacial tension between the two phases in the bulk region. Blood components such as red blood cell ghosts, plasma, and lymphocytes have been shown to have significant effects in experimental models of silicone oil emulsification (Bartov et al. 1992). To confer a similar hydrodynamic effect in these experiments, a synthetic surfactant, TX-100, was used as an emulsifier to lower the interfacial tension from 28 mN/m (for saline-SiOil) to 4.4 mN/m. Experiments were performed above the critical micelle concentration of the surfactant to ensure that surfactant was readily available. Even at this low interfacial tension value, no droplets were formed. The albumin solution gave a lower interfacial tension (2.5 mN/m), but it was difficult to visualize the interface through this liquid as it was cloudy. It should be noted that proteins can stabilize an interface as a result of elastic effects, known to play a role in tear films (Cwiklik 2016). Oils with lower viscosity than used here have been shown in previous work (Heidenkummer, Kampik & Thierfelder 1991; Chan et al. 2015) to support emulsification, but bulk emulsification was not observed here with an oil of low viscosity (500 mPas).

Limitation

The eye chamber is not spherical because of the presence of the lens, but detailed numerical simulations such as those by Abouali et al. (2012) show similar trends in velocity to those employed here. Our tests lasted a few minutes whereas the eye can be in continuous motion. We investigated some extreme saccade conditions to cover 'worst case' scenarios in terms of inertia and acceleration. Patient-related factors such as eye size, presence or absence of surface active species were studied, with parameters and conditions selected to try to cover the different possibilities. Temperature is not expected to play an significant role: the viscosity of the oils at 37°C was measured as 0.41, 0.72 and 3.64 Pa s for A500, B1000 and B5000, respectively, which is similar to those tested, and interfacial tensions are similarly lower. The effect of gravity was assessed by tilting the axis of rotation (up to 30 degrees). This introduced asymmetry to the interface but did not promote droplet formation at the bulk fluid-fluid interface.

This study shows that bulk emulsification did not occur in the model system and is unlikely to arise in the human eye. The observation of droplet formation at the moving contact line indicates that surface emulsification mechanisms are responsible for the formation of droplets. The adhesion of oil at the wall leading to droplet break-up has recently been studied by Lu et al. (2018) in a microchannel device. In this scenario, droplet formation will be determined by the saccade parameters, the ratio of the fluid viscosities, and factors affecting contact line motion including the topology of the surface and species secreted by the cells on the retina wall.

References

Abouali O, Modareszadeh A, Ghaffariyeh A & Tu J (2012): Numerical simulation of the fluid dynamics in vitreous cavity due to saccadic eye movement. Med Eng Phys **34**: 681–692.

Bahill AT, Clark MR & Stark L (1975): The main sequence, a tool for studying human eye movements. Math Biosci **24**: 191–204.

Bartov E, Pennarola F, Savion N, Naveh N & Treister G (1992): A quantitative in vitro model for silicone oil emulsification. Role of blood constituents. Retina **12**(Supplement): S23–S27.

Bonfiglio A, Lagazzo A, Repetto R & Stocchino A (2015): An experimental model of vitreous motion induced by eye rotations. Eye Vis **2**: 10.

Caramoy A, Schroder S, Fauser S & Kirchhof B (2010): In vitro emulsification assessment of new silicone oils. Br J Ophthalmol **94**: 509–512.

Caramoy A, Kearns VR, Chan YK et al. (2015): Development of emulsification resistant heavier-than-water tamponades using high molecular weight silicone oil polymers. J Biomater Appl **30**: 212–220.

Chan YK, Ng CO, Knox PC, Garvey MJ, Williams RL & Wong D (2011): Emulsification of silicone oil and eye movements. Investig Ophthalmol Vis Sci **52**: 9721–9727.

Chan YK, Sy KHS, Wong CY, Man PK, Wong D & Shum HC (2015): In vitro modeling of emulsification of silicone oil as intraocular tamponade using microengineered eye-on-a-chip. Investig Ophthalmol Vis Sci **56**(5): 3314–3319.

Cibis P, Becker B, Okun E & Canaan S (1962): The use of liquid silicone in retinal detachment surgery. Arch Ophthalmol **68**: 590–599.

Cwiklik L (2016): Tear film lipid layer: A molecular level view. Biochim Biophys Acta Biomemb **1858**: 2421–2430.

De Silva DJ, Lim KS & Schulenburg WE (2005): An experimental study on the effect of encircling band procedure on silicone oil emulsification. Br J Ophthalmol **89**: 1348–1350.

Fawcett IM, Williams RL & Wong D (1994): Contact angles of substances used for internal tamponade in retinal detachment surgery. Graefes Arch Clin Exp Ophthalmol **232**: 438–444.

Federman JL & Schubert HD (1988): Complications associated with the use of silicone oil in 150 eyes after retina-vitreous surgery. Ophthalmology **95**: 870–6.

Heidenkummer HP, Kampik A & Thierfelder S (1991): Emulsification of silicone oils with specific physicochemical characteristics. Graefes Arch Clin Exp Ophthalmol **229**: 88–94.

Kanski JJ & Daniel R (1973): Intravitreal silicone injection in retinal detachment. Br J Ophthalmol **57**: 542–545.

Lu Y, Chan YK & Lau LH et al. (2018): Adhesion of silicone oil and emulsification: an in vitro assessment using a microfluidic device and "Eye-on-a-Chip". Acta Ophthalmol **97**: 313-318.

Miller JB, Papakostas TD & Vavvas DG (2014): Complications of emulsified silicone oil after retinal detachment repair. Semin Ophthalmol **29**: 312–318.

Nakamura K, Refojo MF & Crabtree DV (1990): Factors contributing to the emulsification of intraocular silicone and fluorosilicone oils. Investig Ophthalmol Vis Sci **31**: 647–656.

Repetto R, Siggers JH & Stocchino A (2008): Steady streaming within a periodically rotating sphere. J Fluid Mech **608**: 71–80.

Saffman PG & Taylor GI (1958): The penetration of a fluid into a porous medium or Hele-Shaw cell containing a more viscous liquid. Proc Royal Soc London **245**: 312–329.

Wetterqvist C. (2004): Tamponade efficiency of perfluorohexyloctane and silicone oil solutions in a model eye chamber. Br J Ophthalmol **88**: 692–696.

Yoshikawa H et al. (2011): 'Oscillatory Kelvin-Helmholtz instability. Part 2. An experiment in fluids with a large viscosity contrast-Helmholtz instability. J Fluid Mech **675**: 249–267.

Received on January 27th, 2020.
Accepted on June 13th, 2020.

Correspondence:
Ru Wang
Department of Chemical Engineering and Biotechnology
University of Cambridge
Philippa Fawcett Drive
Cambridge CB3 0AS
UK
Tel: (+44)7490 651655
Email: rw565@cam.ac.uk

A PhD studentship for RW from the W.D. Armstrong Fund is gratefully acknowledged. The saccadic motion micro-controller was developed by Mr Sebastien Cosfenoy.

Supporting Information

Additional Supporting Information may be found in the online version of this article:

Appendix S1 Analytical solution to the governing equation of a fluid flow in a sphere under saccades.